13th ewtec 2019 Proceedings of the 13th European Wave and Tidal Energy Conference 1-6 Sept 2019, Naples, Italy

Characterization of in-stream tidal energy resources in the Gulf of California: implementation, calibration and validation of a hydrodynamic model

Anahí Bermúdez-Romero, Vanesa Magar, Markus S. Gross, Victor M. Godínez, Manuel López, Erick Rivera-Lemus

Abstract—**With the aim of evaluating regional and local tidal stream energy resources, we implemented two different models of the Gulf of California (GoC). In both models, we assume that tides within the GoC are generated by co-oscillation with the Pacific Ocean. The first model, GC_6480m, is a shallow water 2D model with a uniform resolution of 6480m throughout the domain. The second model, GC_MD, is a multi-domain model consisting of three, two-way coupled subdomains, with a resolution of 6480m, 2160m, and 240m in the zone with greatest resolution. This greatest resolution subdomain covers two bays located northeast of the GoC: Bahía San Jorge (BSJ) and Bahía Adair (BAd). The data obtained from an Acoustic Doppler Current Profiler (ADCP), installed in June 2017 in BSJ, is used to calibrate and validate the numerical models. The relative error and the root mean square errors was computed for both models at the observation station. The results show there is better agreement between the model and the observations in GC_MD than in GC_6480m. For both models, the error decreases when the Chézy friction coefficient is reduced from its default value of 65 $m^{1/2}/s$, to a value of 45 $m^{1/2}/s$. Once the model has been calibrated, a one-year long simulation is used to generate maps of tidal energy resource indicators, such as the annual mean spring tide maximum speed, the annual mean spring tide maximum Tidal Power Density (TDP), and the Annual Energy Production (AEP). We found maximum values in areas where strong tidal current tunnelling has been observed, such as the Midriff Islands and the channels that form between them and the continent. Horizontal tunnelling occurs in these regions, caused by a decrease in channel width. In the northern region of the Gulf, tidal currents also appear strong, in this case due to vertical tunnelling caused by a decrease in channel depth. The region of vertical tunnelling includes BSJ and BAd.**

Keywords— **Annual energy production, hydrodynamic model, tidal energy resource, tidal power density.**

I. Introduction

TIDAL in-stream energy exploits the kinetic energy generated in the oceans by the interactions between the Earth, the Sun and the Moon, and turns it into mechanical energy, which is then converted into electricity. Tides are fully predictable, giving in-stream power generation a significant advantage over other sources of marine renewable energy. At a local scale, tides are affected by the bathymetry, bottom friction and density gradients. These local effects, together with the currents generated by intermittent meteorological conditions, can lead to significant variations in horizontal and vertical

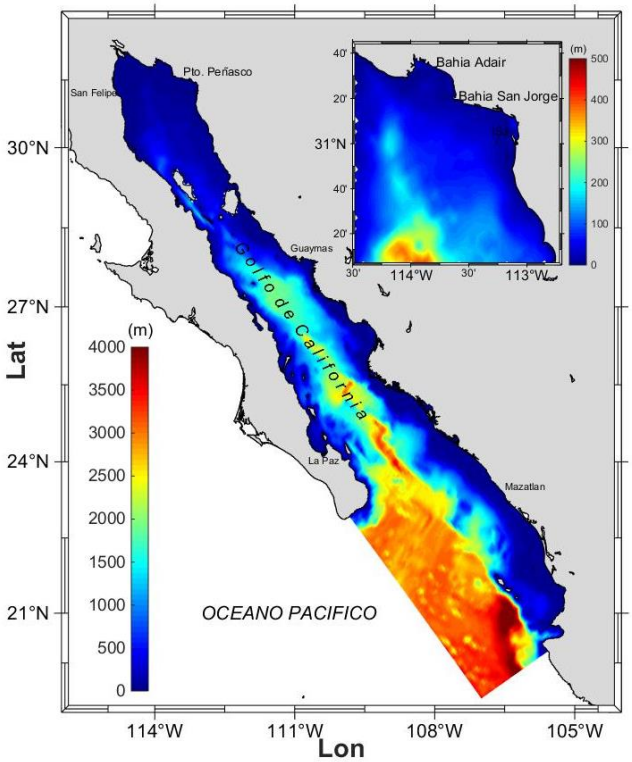

Fig. 1. Region of interest, showing the GEBCO bathymetry used in the numerical models.

This paper was submitted in tidal resource characterization track with the ID 1680. This work was supported in part by the SENER-CONACYT, for 2014-06 period. All authors are with Department of Physical Oceanography, CICESE, Carretera Ensenada-Tijuana 3918, Ensenada, Baja California, México. Their emails are now listed in authorship order: anahi.berom@gmail.com, vmagar@cicese.mx, mgross@cicese.edu.mx, mxcali@cicese.mx, malope@cicese.mx, and elemus@cicese.mx.

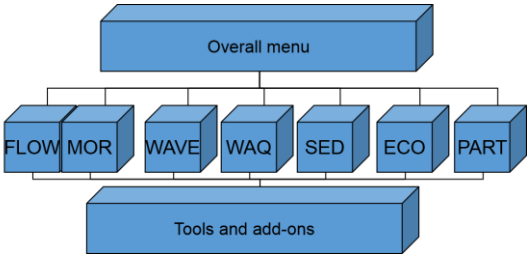

Fig. 2. Schematic of the Delft3D modelling suite and its different modules.

velocity. Therefore, at regional and local scales, fine resolution models that accurately resolve current velocities, in particular close to the coastline, need to be implemented. The resolution needed for both the model and the bathymetry for tidal energy applications, will depend on the development stage of the in-stream project. For regional models, a grid resolution of 5 km or less is acceptable, but as we proceed further in the site characterization, the model grid size needs to be of 500 m or less at the pre-feasibility stage, or 50m or less at the full feasibility and development stages [1].

In the Gulf of California, a marginal sea located in the northwest Mexican coast (see Fig. 1), many studies (both numerical and experimental) have described different oceanographic features, such as trapped coastal waves, coastal upwelling, current and gyre dynamics and tidal mixing. However, so far very few studies have characterized tides in the GoC as a form of renewable energy resource. Such characterization, in order to be of relevance for developers and end-users, requires the research to focus on the analysis of a number of parameters, variables, and indicators of relevance for marine renewable energy, which ultimately will lead to a realistic estimate of the AEP, i.e, the projected annual energy production [2].

II. MATERIALS AND METHODS

A. *Delft3D-Flow numerical model*

Delft3D-Flow is one of the modules of the Delft3D modelling suite, developed by Deltares. The modelling suite consists of the following modules: flow-morphodynamics; waves; water quality; sediment dynamics; ecology; and particle tracking. Delft3D can simulate shallow water flows, sediment transport and morphodynamic processes, and biogeochemical tracer dynamics in coastal and estuarine areas. Tidal and meteorological forcings can be implemented on curvilinear grids which are topologically Cartesian in nature, but can be fitted to coastal boundaries and improve the model predictions in coastal regions. In 3D simulations, the vertical grid is defined using the terrain following, σ co-ordinate approach. A schematic of the modelling suite is shown in Fig. 2 [3].

In shallow water, 2D flows, forced by tidal constituents at the open boundaries, the system of equations consists of two momentum conservation equations for the horizontal components of the velocity, a conservation equation for the hydrostatic pressure, and the continuity (mass conservation) equation, as follows:

$$\frac{\partial U}{\partial t}+U\frac{\partial U}{\partial x}+V\frac{\partial U}{\partial y}+\frac{\omega}{\zeta+d}\frac{\partial U}{\partial \sigma}-fV = -\frac{1}{\rho_0}\frac{\partial P}{\partial x}+F_x+M_x+\nabla.(D_H\nabla V)+\tau_{sx}-\tau_{bx}$$

$$\frac{\partial V}{\partial t}+U\frac{\partial V}{\partial x}+V\frac{\partial V}{\partial y}+\frac{\omega}{\zeta+d}\frac{\partial V}{\partial \sigma}-fU = -\frac{1}{\rho_0}\frac{\partial P}{\partial y}+F_y+M_y+\nabla.(D_H\nabla V)+\tau_{sy}-\tau_{by}$$

$$\frac{P}{\rho_0}=g\nabla\zeta, \text{ and}$$

$$\frac{\partial \zeta}{\partial t}+\frac{\partial[(\zeta+d)U]}{\partial x}+\frac{\partial[(\zeta+d)V]}{\partial y}=0,$$

where ζ is the water level measured from the reference level corresponding to mean sea level (MSL), d is the water depth from MSL, defined as positive downwards, $\overrightarrow{U}=(U,V)$ is the depth-averaged velocity, S represents mass source/sink terms, $P=(P_x,P_y)$ is the pressure gradient, $\overrightarrow{F}=(F_x,F_y)$ the horizontal Reynolds stresses, $\overrightarrow{M}$ are the external forcing terms, D_H is the depth-averaged horizontal turbulent eddy viscosity, and $\tau_s-\tau_b$ represents the difference between the surface and the bottom shear stresses, respectively.

B. *Model configuration*

Two hydrodynamic models were implemented in the Gulf of California with the aim of evaluating the regional and local tidal stream energy: GC_6480m is a 2D model with 6480m of resolution; and GC_MD is a 2D multi-domain model of variable resolution, with a mesh of 6480m at the western approach and the mouth of the Gulf of California, a mesh of 2160m in the coastal regions and the north part of the Gulf, and a fine resolution of 240m covering Bahía Adair and Bahía San Jorge, two bays located in the Northeastern part of the Gulf.

The bathymetry of each domain was obtained from the General Bathymetric Chart of the Oceans (GEBCO), a bathymetry with a resolution of 30 arcseconds, which is equivalent to approximately 928m. The interpolation of the bathymetry into the model grids was performed using grid cell averaging, triangular interpolation, or internal diffusion, depending on the number of bathymetric data points within the grid cells.

The model was forced at the open boundary with 13 principal tidal harmonics (M2, S2, N2, K2, K1, O1, P1, Q1, MF, MM, M4, MS4, MN4), obtained from TPXO8.1 (through Delft Dashboard), a Global Inverse Tidal Model [4, 5]. Tides in the GoC are generated by co-oscillation with

the Pacific Ocean and they are one of the most important oceanographic features in the region.

For a more accurate representation of the flow velocity in the study area, the model parameters such as the reflection parameter, the horizontal viscosity and the friction coefficient (Chézy) were calibrated. A correlation coefficient and the Root Mean Square Error (RMSE) were used to assess the agreement between the model and ADCP observations obtained at the location (31°00'44.6" N, 113°14'11.4" W), about one kilometre east of Isla San Jorge. Model and observations at 30 minute intervals were used for the model-measurement intercomparisons.

C. *In-situ measurements and comparisons with model predictions*

An Acoustic Doppler Current Profiler (ADCP) was installed in San Jorge Bay, located northwest of the Gulf, to measure the flow velocity and validate the two models. Approximately 6 months of data (from 1 June 2017 to 26 November 2017) have been collected at the site, of which one month was used to compare and calibrate the numerical modelling outputs with observations of vertically averaged velocities. A number of statistical indicators were used to identify the model that showed agreement with the flow speed measurements. Different indicators were assessed, including: the mean relative error of the model flow speeds, u_{mod} and u_{obs}, over a total of N discrete time-series data points over one month. The mean relative error for the speeds, MRE_U, is defined as:

$$MRE\_U = \frac{1}{N}\sum_{i=1}^{N}\frac{u_{mod,i} - u_{obs,i}}{u_{obs,i}}$$

The mean relative error for the tidal power density (TPD), MRE_P, defined as:

$$MRE\_P = \frac{1}{N}\sum_{i=1}^{N}\frac{u_{mod,i}^3 - u_{obs,i}^3}{u_{obs,i}^3}$$

The same criteria are applied to the maximum speed on spring tides, over one month (either one or two spring tide maxima, depending on the month initial and end dates), and over a full year (around 22 to 26 spring tide maxima over one year). The root-mean-square error, $RMSE$, is also computed. For the speeds, $RMSE\_U$, it is defined as:

$$RMSE\_U = \sqrt{\frac{1}{N}\sum_{i=1}^{N}\frac{u_{mod,i}^2 - u_{obs,i}^2}{u_{obs,i}^2}}$$

We also compute the RMSE associated with TPD, the $RMSE\_P$, with in terms of the TPD defined as:

$$RMSE\_P = \sqrt{\frac{1}{N}\sum_{i=1}^{N}\frac{TPD_{mod,i}^2 - TPD_{obs,i}^2}{TPD_{obs,i}^2}}$$

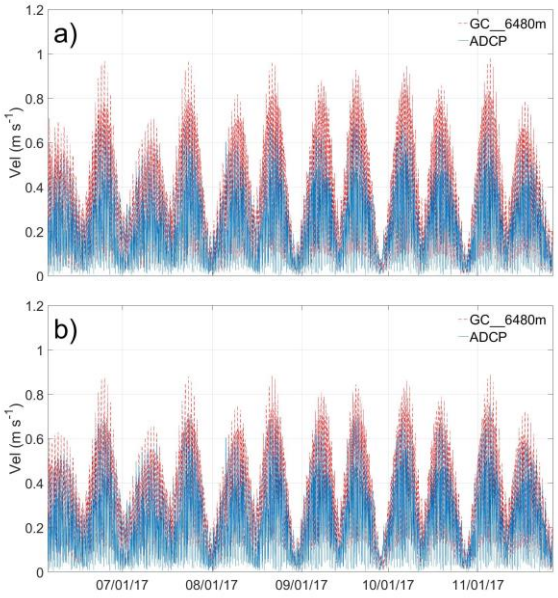

Fig. 3. ADCP measurements and model time series at ADCP location, with the *GC_6480m*$_{Chezy65}$ (a) and the *GC_6480m*$_{Chezy45}$ (b) models and Chézy parameterizations.

and the Annual Energy Production (AEP). The TPD and the AEP are defined as

$$TPD = \frac{1}{2}\rho u^3, \text{and} \quad (1)$$

$$AEP = \frac{1}{N}\sum_{i=1}^{N} TPD_i \quad (2)$$

respectively.

Several variations of these indicators can be computed, here we focus on mean maximum spring tide maxima for the speed u (in m/s), for the TPD (in W/m² or kW/m²) , and on the expected AEP (in kWh/year), the annual energy production over one year based on hourly data.

TABLE I
MEAN ANNUAL SPEEDS: MODEL-DATA COMPARISONS

	Correlation coefficient	RMSE (m/s)
GC_6480m$_{Chezy65}$	0.795	0.18
GC_6480m$_{Chezy45}$	0.816	0.16
GC_MD$_{Chezy65}$	0.871	0.16
GC_MD$_{Chezy45}$	0.885	0.10

III. RESULTS AND DISCUSSION

E. *Model calibration and validation*

Table I shows the correlation coefficient and the $RMSE$ between model and observations for the two models and the two values of C_f considered, i.e., with C_f= 45 m$^{1/2}$/s and C_f= 65 m$^{1/2}$/s. The statistical analysis shows a decrease in the error through calibration of C_f (Chézy). Other model

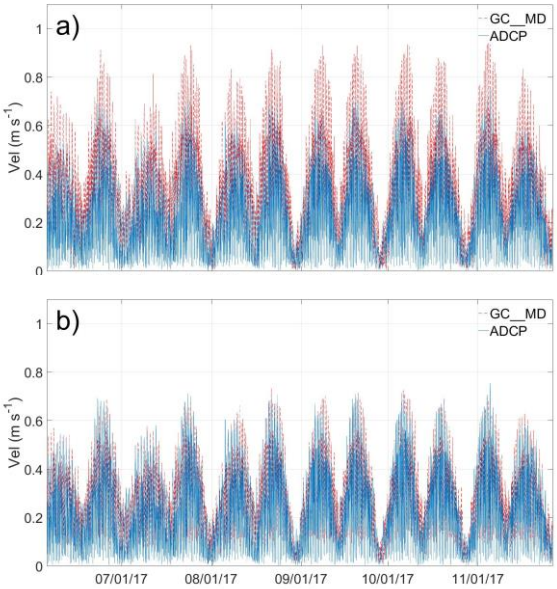

Fig. 4. ADCP measurements and model time series at ADCP location, with the GC_MDChezy65 (a) and the GC_MDChezy45 (b) models and Chézy parameterizations.

parameters were also tested (e.g., the horizontal viscosity, and the reflexion coefficient), but only variations of the friction coefficient had a significant effect on the predictions. This is as expected, based on results shown by [6]. In GC_6480m, although the difference between the coefficient error may seem insignificant, the RMSE (0.16 m/s) is smaller. On the other hand, the multi-domain model GC_MD shows a better correlation and a smaller RMSE (0.11 m/s) with a Chézy value of C_f = 45 m$^{1/2}$/s. Figures 3 and 4 show the data comparison of the GC_6480m and GC_MD respectively. Although we found a good agreement between the numerical and experimental time series, the numerical results in some tidal cycles seem to overestimate the flow speed.

Overall the model results show a better agreement with C_f= 45 m$^{1/2}$/s, considering that a smaller $RMSE$ will provide more accurate estimates of tidal energy resource indicators. The results, however, have a relatively high $RMSE$ of 0.1 to 0.2 m/s. This will be reflected in large errors for the TPD and the AEP . For example, with the $GC\_MD_{Chezy45}$ model, MRE_U is of 5%, but MRE_P is 15%, three times larger. Since the correlation and the $RMSE\_U$ are lowest for the $GC\_MD_{Chezy45}$ model, this model is used in subsequent analyses.

We assume that using one point for validation is enough to trust the results of $GC\_MD_{Chezy45}$ in the domain covered by the greatest scale model. For regions outside that domain, however, it is necessary to perform more model-data comparisons at other locations and to adjust the model parameterizations, for best results. This would require the generation of friction coefficient maps, to reflect the spatial variations of C_f.

Figure 5 shows the annual mean of the spring tide maximum speeds for the *GC_6480m* (left) and the *GC_MD* (right) model, with C_f= 45 m$^{1/2}$/s. The *GC_MD* model with a resolution of 240m in the area of interest helps identify the regions where this indicator is largest. The areas with largest speeds are better defined in the *GC_MD* model due to the increase in grid resolution, but the general locations agree well between models. The bathymetry has a strong influence on the flow velocity, so a resolution in the bathymetry that is finer to the one we have used is necessary, in order to reduce uncertainty about the location of optimal sites, and increase the precision when evaluating the energy resource.

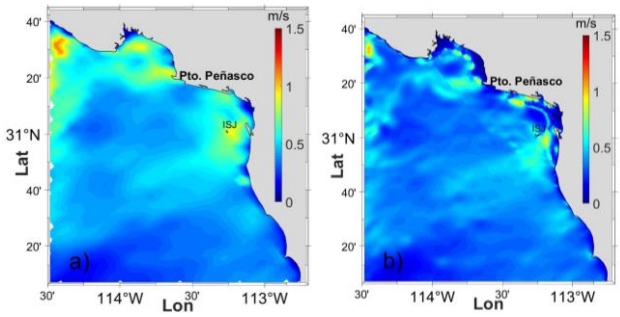

Fig. 5. Annual mean spring tide maximum speeds, (a) GC_6480m y (b) GC_MD.

Figure 6 shows the mean *TPD* obtained from the spring tide maximum TPDs over one year. The geographical locations with maxima TPD are better defined at scales of 240m, and some of them are not resolved with the 6840m model, but in general there is good agreement between the two models. A better spatial resolution, however, is more useful in tidal energy resource characterizations because it allows field researchers to identify locations where an ADCP is worth installing, based on the model predictions. Indeed, although the models are very helpful for the generation of maps and atlases, there is still a need for local measurements to be performed, not only for model calibration and validation, but also for *in-situ* monitoring of oceanographic and environmental conditions. The left inset of Fig. 6, for example, shows clearly defined areas, four in Bahía Adair (to the Northwest of Puerto Peñasco), and two in Bahía San Jorge (one south of the Morúa coastal lagoon, and one in the vicinity of ISJ), which could be instrumented for in-situ data collection and analysis. This could complement and inform numerical modelling, both at local and regional scales. Figures 5 and 6, show that the annual mean speed and the mean annual *TPD*, respectively, over spring tides, are good site selection criteria in macrotidal environments, better than the mean annual speed or mean annual *TPD*.

Figure 7 shows the estimated annual energy production (AEP) map. To generate the estimated AEP maps, the $GC\_6480m_{Chezy45}$ and the $GC\_MD_{Chezy45}$ models were run for a full year, then the values of the TPD at hourly time intervals were determined, and then they were averaged over the year. The resulting AEP is expressed in kWh/m^2. It is clear that the sites with best resources can be identified using the AEP as a renewable energy resource indicator.

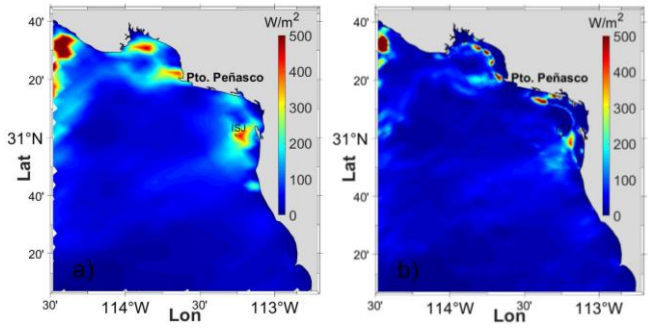

Fig. 6. Mean Tidal Power Density (TPD) over spring tide maximum speeds, (a) GC_6480m y (b) GC_MD.

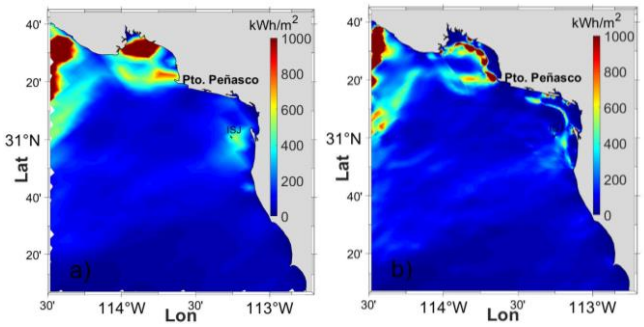

Fig. 7. Annual Energy Production (AEP), (a) GC_6480m y (b) GC_MD.

The sites corresponding to largest AEP coincide with the sites corresponding to largest mean TPD over the yearly spring tide speed maxima, but the AEP has more spatial spreading. Finally, we observe some areas in Bahía Adair and in the Colorado Delta Approach (to the Northwestern side of the study domain), that have AEP in the order of 1000 kWh/m^2.

These results need to be tested, in a follow-on study, against other numerical simulations performed with in-situ or remotely sensed bathymetric data, i.e., with a bathymetry that has higher resolution that the GEBCO bathymetry used here. Also, it is important to note that these AEP values are low compared to those in sites that are appropriate for first generation tidal energy devices. For such sites, the maximum speeds in spring tides are expected to be above 2 m/s. Therefore, significant research time and skills need to be developed to accelerate, in turn, the development of technologies that can exploit tidal energy resources at low flow speeds.

ACKNOWLEDGEMENT

This research was supported by SENER-CONACYT under grant No. 249795. We thank all the people that participated in this work, both data processing and work field.

REFERENCES

[1] C. Legrand, "Assessment of Tidal Energy Resource," European Marine Energy Centre Ltd (EMEC) Marine Renewable Energy Guides, Scotland, vol. 4, 60 p., 2009.

[2] K. Haas, Z. Defne, X. Yang, and B. Bruder, "Hydrokinetic Tidal Energy Resource Assessments Using Numerical Models," in *Marine Renewable Energy*, Springer, Cham, 2017, pp. 99-120.

[3] D. Hydraulics, "Delft3D-FLOW User Manual: Simulation of multi-dimensional hydrodynamic flows and transport phenomena. including sediments", Deltares, Rotterdamseweg, 2018.

[4] G. D. Egbert, A. F. Bennett, and M. G. Foreman, "TOPEX/POSEIDON tides estimated using a global inverse model," *J. Geophys. Res*., vol. 99, pp. 24821-24852, 1994.

[5] G. D. Egbert, and S. Y. Erofeeva, "Efficient Inverse Modeling of Barotropic Ocean Tides," *J. Atmos. Oceanic Technol*., vol. 19, pp. 183-204, 2002.

[6] S. Baston, S. Waldman, and J. Side, "Modelling energy extraction in tidal flows," *MASTS Position Paper*, vol. 1, 2015. [Online] Available: http://www.masts.ac.uk/media/126430/140828_position_paper_tidal_ energy_extraction_rev2